JCTC Journal of Chemical Theory and Computation

Article

pubs.acs.org/JCTC

Path Integral Coarse-Graining Replica Exchange Method for Enhanced Sampling

Yuxing Peng,[†] Zhen Cao,[†] Ruhong Zhou,[‡] and Gregory A. Voth*,[†]

[†]Department of Chemistry, James Franck Institute, and Computation Institute, The University of Chicago, 5735 South Ellis Avenue, Chicago, Illinois 60637, United States

[‡]Computational Biology Center, IBM Thomas J. Watson Research Center, Yorktown Heights, New York 10598, United States

ABSTRACT: An enhanced conformational space sampling method is developed that utilizes replica exchange molecular dynamics between a set of imaginary time Feynman path integral replicas, each having an increasing degree of contraction (or coarse-graining) of the quasi-particle or "polymer beads" in the evaluation of the isomorphic ring-polymer potential energy terms. However, there is no contraction of beads in the effectively harmonic kinetic energy terms. The final replica in this procedure is the fully contracted one in which the potential energy is evaluated only at the centroid of the beads—and hence it is the classical distribution in the centroid variable—while the initial replica has the full degree (or even a heightened degree, if desired) of quantum delocalization and tunneling in the physical potential by the polymer necklace beads. The exchange between the different ring-polymer ensembles is governed by the Metropolis criteria to guarantee detailed balance. The method is applied successfully to several model systems, ranging from one-dimensional prototype rough energy landscape models having analytical solutions to the more realistic alanine dipeptide. A detailed comparison with the classical temperature-based replica exchange method shows an improved efficiency of this new method in the classical conformational space sampling due to coupling with the fictitious path integral (quantum) replicas.

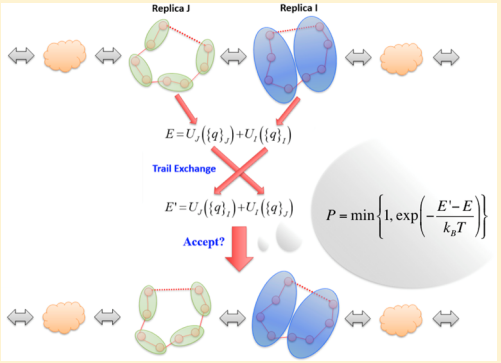

1. INTRODUCTION

Efficient sampling is essential in molecular dynamics (MD) simulation. Indeed, despite the many successes of classical MD simulations (see, e.g., refs 1−4), the method often suffers from insufficient sampling due to the complexity of the energy landscape of realistic systems. This complexity is due to the potential energy function having many different energy basins separated by barriers of several (or many) times k_BT (where k_B is the Boltzmann constant). This situation has led to ongoing and extensive efforts to further improve the sampling efficiency of classical MD. Among these efforts, one methodology is to bias the Hamiltonian of the system under study. Some successful examples include umbrella sampling[5,6] and the metadynamics method.[7] Prior knowledge of the system is often required in either approach to define a finite number of collective variables for the enhanced sampling, and biasing potentials are then added either statically (as "windows") in umbrella sampling or dynamically as (as Gaussian "hills") along the trajectory in time as done in metadynamics to help the system escape the basins in the potential energy surface. Using approaches such as the weighted histogram analysis method in umbrella sampling,[8,9] a targeted potential of mean force (PMF) along the chosen collective variables can then be obtained from the simulation trajectories. Another category of methods such as steered MD[10] or simulated annealing[11] introduce parameters to combine two types of potential energies, and reweighting methods are then needed to obtain the PMFs for important regions.

Alternative means to achieve sufficient MD sampling are based on a modification of the ensembles. Recently, the temperature accelerated molecular dynamics[12] (TAMD) was reported to enhance the sampling at a given physical temperature by coupling a higher temperature Langevin thermostat to the auxiliary collective variables. Together with the single sweep method,[13] TAMD can be used to investigate the free energy landscape of certain complex macromolecular systems.[14] Another frequently used method is the parallel tempering method, or replica exchange molecular dynamics (REMD).[15] In this method independent replicas of the system at different temperatures are run together. Attempts are made periodically to exchange configurations between adjacent replicas based on the Metropolis criteria to guarantee detailed balance within any given ensemble. The replica having the targeted temperature can accept configurations obtained from the higher temperature replicas, which will help to overcome the energy barriers and thus access the microstates at other energy basins otherwise difficult to reach by MD at the lower target temperature. The REMD method has often proven to be an effective way to obtain the converged properties of the equilibrium distributions,[16,17] and different variants, such as Hamiltonian REMD (HREMD)[18−21] and reservoir REMD (RREMD),[22−24] have been developed.

Received: May 23, 2014
Published: July 25, 2014

   dx.doi.org/10.1021/ct500447r | J. Chem. Theory Comput. 2014, 10, 3634−3640

On the other hand, in terms of the known laws of physics, enhanced sampling of conformational space is naturally achieved in quantum mechanics via well-known quantum effects such as delocalization of the quantized motion and tunneling. In principle, exploiting this physics as a means to *enhance classical MD sampling* could provide a fruitful alternative (or an auxiliary add-on) to classical MD, REMD, and other enhanced MD sampling methods. In this paper, it will be shown that this goal can be achieved via a relatively simple contraction, or coarse-graining, scheme applied to path integral MD (PIMD) replicas in the discretized imaginary time Feynman path integral (the isomorphic classical ring-polymer of "beads") formulation of quantum statistical mechanics. A set of path integral ring-polymer replicas, each having an increasing degree of bead contraction in the potential energy evaluation but not in the kinetic energy (harmonic chain) terms, can be readily implemented into an REMD scheme. The first replica in this approach is the fully delocalized and tunneling path integral ring-polymer consisting of a number of beads P, while the final replica also has P beads but *has the potential energy function evaluated only at the centroid of the P ring-polymer beads*. Importantly, the latter provides the classical distribution function in the centroid variable since the collective harmonic spring term of the path integral ring-polymer is independent of the centroid variable. As a result of this approach, which we call the path integral coarse-graining replica exchange MD (PICG-REMD) method, each replica of P beads gradually gains or loses quantum effects arising from the interaction with the physical potential for the simulated system. The simulation performed in the most quantum ensemble can fully tunnel through the energy barriers, while these effects are coupled via the intermediate replicas to the final replica obeying classical statistical mechanics in its centroid distribution.

It should be noted that similar ideas, based on quantum staging path integral Monte Carlo sampling, have been proposed previously in the "quantum annealing" approach,[25−27] to search for the global minimum of a given energy landscape. In each cycle of the quantum annealing, the quasi-particles, including the kinetic energy beads, are gradually reduced, and finally the system reaches the classical limit of a single bead. In the present work, the PICG-REMD method uses the coarse-graining concept for the evaluation of the potential terms in the ring-polymer mapping, while retaining all of the beads in the ring-polymer kinetic energy terms for every replica. In other words, the number of quasi-particles is the same in all replicas; however, the evaluation of the potential energy terms of the replicas changes from the quantum limit to the classical limit.

The remainder of this paper is organized as follows: a detailed discussion of the physical motivation behind the PICG-REMD method and how to build the hierarchy of the replica exchange ensembles will be presented in Section 2. Systematic tests of this methodology, including one-dimensional (1-D) cases and alanine dipeptide will be presented in Section 3. Simulation results will also be compared in some cases with those obtained from temperature-based REMD to highlight the features of PICG-REMD. In Section 4, concluding remarks will be presented.

2. THEORETICAL AND COMPUTATIONAL METHODS

2.1. Normal Mode Path Integral Molecular Dynamics.

In this subsection, the numerical implementation of Feynman's path integral formulation of quantum statistical mechanics[28] via the PIMD method will be briefly reviewed, and the application of this method utilizing the normal mode representation will be discussed. To capture the quantum effects, the PIMD method simulates the discretized imaginary time path integral as classically isomorphic rings of quasi-particles, or "beads." The number of beads is equal to the number of discrete imaginary time slices of the path integral, given by a parameter P. In PIMD the propagation of each bead is driven by the classical force field (divided by the number of beads) in real space as well as the spring-potential from adjacent beads within the same isomorphic ring-polymer. The latter spring term arises from the imaginary time propagation of the free particle, that is, the kinetic energy. It can be shown that the quantum partition function is isomorphic with the classical partition function for the ring-polymer in the canonical ensemble in the limit that the number of beads P becomes large. Thus, if the number of beads for a real particle is P, the quantum partition function for the particle system can be calculated by

$$Q = \int \mathrm{d}p_1 \mathrm{d}p_2 \cdots \mathrm{d}p_P \int \mathrm{d}x_1 \mathrm{d}x_2 \cdots \mathrm{d}x_P \exp(-\beta H_{\mathrm{eff}}) \tag{1}$$

and the Hamiltonian of the system, H, can be written as

$$H_{\mathrm{eff}} = \sum_{i=1}^{P} \left[\frac{p_i^2}{2m'} + \frac{mP}{2\beta^2\hbar^2}(x_i - x_{i+1})^2 + \frac{1}{P}V(x_i) \right] \tag{2}$$

where m is the mass of the particle, and β is $1/k_{\mathrm{B}}T$. Notation is used here for a single particle in one-dimension without lack of generality.

Conventional PIMD simulations can suffer from inefficient sampling, and different approaches have been developed to overcome this problem. One popular choice is to conduct normal mode path integral molecular dynamics (NMPIMD),[29,30] in which the coordinates of the isomorphic ring are transformed into the normal mode representation. The Hamiltonian of the system in NMPIMD can be rewritten as

$$\begin{aligned} H_{\mathrm{eff}} &= \sum_{k=1}^{P} \left(\frac{p_{u_k}^2}{2m_{u_k}} + \frac{mP}{2\beta^2\hbar^2}\lambda_k {u_k}^2 + \frac{1}{P}V[x_k(u)] \right), \\ \lambda_1 &= 0,\ \lambda_P = 4P, \\ \lambda_{2l-1} &= \lambda_{2l-2} = 2P\left[1 - \cos\left(\frac{2\pi(l-1)}{P}\right)\right]. \end{aligned} \tag{3}$$

where u represents the normal mode coordinate, which can be converted through the transformation matrix $C^{(P)}$:

$$u_j = \frac{1}{P}\sum_{i=1}^{P} C_{ji}^{(P)} x_i \tag{4}$$

where

$$C_{ji}^{(P)} = \begin{cases} 1 & j = 1 \\ -\sqrt{2}\sin\dfrac{2\pi(l-1)i}{P} & j = 2l-2 \\ \sqrt{2}\cos\dfrac{2\pi(l-1)i}{P} & j = 2l-1 \\ (-1)^i & j = P \end{cases} \tag{5}$$

In the equation above, l is from 2 to $P/2$, and P is chosen to be even (see Section 2.3).

dx.doi.org/10.1021/ct500447r | J. Chem. Theory Comput. 2014, 10, 3634−3640

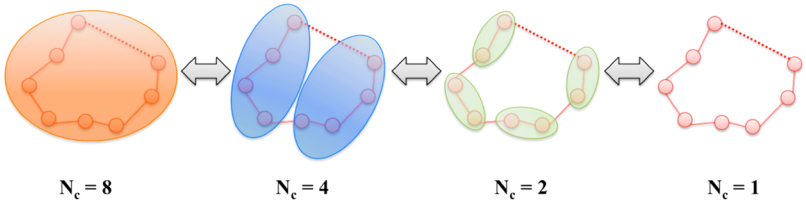

Figure 1. Illustration of the "coarse-graining" scheme for $P = 8$ quasi-particle beads of the isomorphic path integral ring-polymer at different contraction levels. These contracted variables are used to evaluate the PIMD ring-polymer potential energy terms via eq 8. Note that the second term in the right-hand side of eq 8 is the full (uncontracted) ring-polymer for the kinetic energy terms. The leftmost panel of the figure shows the $N_c = 8$ representation of the centroid (or classical) replica, while the rightmost one represents the $N_c = 1$ representation of the replica with the full quantum effects.

The time propagation is done in the NM representation, and a chain of M Nose−Hoover thermostats are linked to each dimension of every normal mode. The zero-frequency mode, corresponding to the centroid motion of the isomorphic ring, is assigned with the real mass of the atom. The fictitious masses of other modes are assigned to be $m_{u_k} = \lambda_k m$ so that they all have the same frequencies. This scheme helps to overcome the "stiffness" problem[29,30] of PIMD and enables efficient samplings.

2.2. Hamiltonian Replica Exchange Molecular Dynamics. In conventional REMD methods, multiple simulations (referred to as "replicas") are run independently under different temperatures. After a certain time interval, an exchange of configurations between two adjacent replicas is tested and accepted obeying the Metropolis criteria. Similarly, this method can be applied for ensembles governed by different Hamiltonians. In that case, the probability of accepting the exchange of the configurations X_I and X_{II} in different ensembles A and B can be calculated as

$$P_{A\leftrightarrow B} = \min\left\{1, \exp\left(-\frac{\Delta E}{k_B T}\right)\right\} \tag{6}$$

where $\Delta E = [H_A(X_{II}) + H_B(X_I)] - [H_A(X_I) + H_B(X_{II})]$ is the change of the total energy after switching the configurations.

2.3. Path Integral Coarse-Graining Replica Exchange Molecular Dynamics. The PICG-REMD method employs the concept of the HREMD, and constructs independent replicas representing different levels of coarse-grained quantum effects. The possibility of accepting an exchange attempt between different replicas is also governed by the Metropolis acceptance criteria. In this section, the discussion is mainly focused on two problems, namely, how to construct each replica in PICG-REMD and how to efficiently exchange the configurations in different replicas to improve the sampling efficiency.

The replicas in the PICG-REMD are constructed by introducing the concept of the "contraction level" N_c, which is used to enable the gradual transition of the quantum coarse-grained annealing by evaluating the potential terms $V(x)$ in the PIMD ring-polymer only through these contracted variables. A common choice of P is usually 2^n, and a set of possible choices of the contract levels can be 2^t, where t is the integer number from 0 to $\log_2 P$ (Figure 1). The coordinates of P quasi-particle beads are then converted into P/N_c contracted variables,

$$x_I^{(N_c)} = \frac{1}{N_c} \sum_{i=(I-1)\times N_c+1}^{I\times N_c} x_i \tag{7}$$

where I represents the index of the new contracted coordinates ranging from 1 to P/N_c. Then the effective PIMD potential of the replica N_c can be written as,

$$V_{eff} = \frac{N_c}{P} \sum_{I=1}^{P/N_c} V(x_I^{(N_c)}) + \sum_{i=1}^{P} \frac{mP}{2\beta^2\hbar^2}(x_i - x_{i+1})^2 \tag{8}$$

Two specific contraction levels are of particular interest here: the first level is for $N_c = 1$, which corresponds to the standard fully quantum NMPIMD method, and the other one is for $N_c = P$, which represents the zero-frequency normal mode u_1 (or centroid) of the isomorphic polymer-ring, that is, the classical system. The corresponding contracted effective Hamiltonian in the latter case can be rewritten as,

$$\begin{aligned} H_{eff} &= \left[\frac{p_{u_1}^2}{2m} + V(u_1)\right] + \sum_{k=2}^{P}\left(\frac{p_{u_k}^2}{2m_{u_k}} + \frac{mP}{2\beta^2\hbar^2}\lambda_k u_k^2\right) \\ &= H_{eff}^0 + H_{eff}^{\Delta} \end{aligned} \tag{9}$$

A significant point of the above equation is that the motion of the centroid mode u_1 is totally decoupled from other normal modes and *samples the classical potential energy surface*. The Hamiltonian H_{eff}^0 is therefore equivalent to that in a classical system with some extra (irrelevant and uncoupled) harmonic normal modes. It is therefore important to note that the upper limit and lower limit of the contraction levels recover the ensembles of the fully quantum and classical systems, respectively. Different contraction levels in the potential evaluation form a series of ensembles that gradually change from the quantum limit to the classical limit forming the basis of this new approach to HREMD.

In practice, a replica can be exchanged with the upper contraction levels gradually increasing its quantum effect, sampling the quantum configurational distribution and possibly escaping from a given free energy basin, and later exchange back to the lower contraction levels sampling the classical configurational distribution as a form of quantum sampling. Analogous to the HREMD methodology, the bottom (classical) replica is used for the sampling and analysis of the equilibrium configurational distributions, and all the other replicas are used to enhance the sampling efficiency of the bottom replica. In other words, the quantum replicas are in many ways fictitious, in that they utilize the effects of quantum mechanics to enhance the sampling. In that regard, they do not need to be the actual physical quantum effects for the problem at hand. Indeed, the additional replicas can have very large enhanced quantum effects to improve the sampling.

An important issue in HREMD simulations concerns how to obtain sufficient exchange ratios, which usually requires a large

dx.doi.org/10.1021/ct500447r | J. Chem. Theory Comput. 2014, 10, 3634−3640

number of transit replicas, whose potential energies can have sufficient overlap in their probability distributions between neighboring replicas. In the PICG-REMD scheme, these replicas can be created by using linear combination of two contraction levels when necessary. Then, the contracted variables can be described by

$$x_{I,\alpha}^{(N_c)} = (1-\alpha)x_I^{(N_c)} + \alpha x_{I'}^{(2N_c)} \tag{10}$$

where α can be any value between 0 and 1, and

$$I' = \begin{cases} I/2 & I \text{ is even} \\ (I+1)/2 & I \text{ is odd} \end{cases} \tag{11}$$

These replicas can provide enough overlap between different replicas to improve the exchange events and obtain better sampling efficiency.

3. RESULTS AND DISCUSSION

3.1. One-Dimensional Oscillator. The sampling of the 1-D oscillator under the perturbation of given external potentials is widely used to explore the behavior of new enhanced sampling methods, because such problems are easy to validate by comparing with the exact analytical solution. Following previous studies[31,32] we monitor the quantity

$$\chi(t) = \int \mathrm{d}x[\rho(x,t) - \rho_B(x)]^2 \tag{12}$$

where $\rho(x,t)$ is defined as the distribution of the oscillator positions x_t collected from the start to the simulation time t, and $\rho_B(x)$ is the analytical solution obtained from Boltzmann distribution. The $\chi(t)$ measurement can be used to determine the quality of convergence and evaluate the sampling efficiency of a new method.

The first prototypical system is an asymmetric double-well potential defined as

$$V(x) = Ax^2 + Bx^3 + Cx^4 \tag{13}$$

where, $A = -70.0$ kcal mol^{-1} Å^{-2}, $B = 1.0$ kcal mol^{-1} Å^{-3}, and $C = 250.0$ kcal mol^{-1} Å^{-4}.

The asymmetric double-well potential is a commonly used model for theoretical studies, such as in transition-state theory for chemical kinetics. The mass of the oscillator was chosen to be the same as the hydrogen atom, and temperature was chosen to be 300 K. The prototypical system possesses two energy minima with the difference of 1.0 kcal mol^{-1} and separated by an energy barrier of ~5.0 kcal mol^{-1}, which is difficult for conventional, classical MD simulations to overcome. It is shown in Figure 2 that only ~24% of the probability distribution (black line) has matched the reference distribution in the first one million time steps, while over a 50 million-step trajectory, the zigzag difference curve shows a very long tail. It is notable that for the conventional MD simulations the oscillator can be trapped in one basin, while the large jumps in the curve represent the oscillator passing through the "transition state" and moving to the other free energy basin.

For comparison, the replica of the classical (centroid) contraction in PICG-REMD simulations (red line) is also shown in Figure 2. Significant improvement can be seen for the PICG-REMD simulation: the difference matches the analytical benchmark by ~95% within 2 million steps, and it approaches to 0 within 10 million steps. It is also observed that the decay of the quantity $\chi(t)$ in the PICG-REMD sampling is relatively

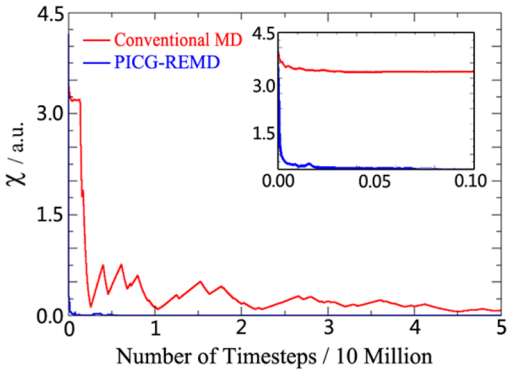

Figure 2. Convergence quantity χ for the first 50 million time steps of the simulations of the 1-D asymmetrical double-well potential. The χ value from PICG-REMD (blue) decays much faster than that from the conventional MD (red). (inset) The comparison of two χ quantities for the first one million time steps.

smooth, which indicates the quantized oscillator can "tunnel" through the energy barriers and assist the classical oscillator in obtaining a good sampling of the underlying potential energy function. Shown in Figure 3 are the system position trajectories

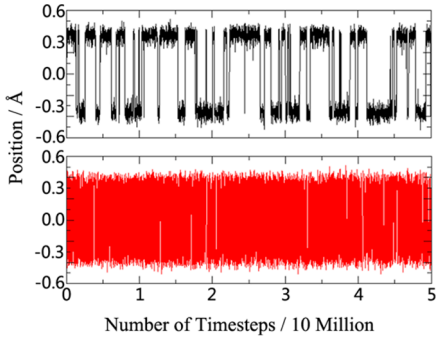

Figure 3. Position of the particle under the 1-D asymmetric double-well potential from the conventional MD (black) and the bottom "classical" replica of the PICG-REMD (red) indicates a more frequent transition across the energy barriers in the PICG-REMD simulations.

from the conventional MD simulation and the classical (centroid or bottom) replica of the PICG-REMD simulation. In the conventional MD trajectory, the system remains trapped in one of the two basins most of the time, and the crossing events between them are rare. However, in PICG-REMD the swapping of the positions between the two basins was very frequent as assisted by the quantum tunneling.

The second test was performed for a more complicated 1-D symmetrical potential energy surface constructed from a sum of Fourier cosine waves from 0.0 to 10.0 Å, similar to the 1-D potential used by Zhou and Berne in a previous study on the smart walking (S-Walking) method:[32]

$$V(x) = \begin{cases} \sum_{i=1}^{10} c_i \cdot \cos\left(\frac{i\pi x}{10}\right) & 0 \le x \le 5 \\ V(10-x) & 5 < x \le 10 \end{cases} \tag{14}$$

A plot of this potential energy and its corresponding Boltzmann distribution are shown in Figure 4. This rough potential has multiple energy minima and barriers, with the largest energy barrier of ~4.5 kcal mol^{-1}. The sampling capability

dx.doi.org/10.1021/ct500447r | J. Chem. Theory Comput. 2014, 10, 3634−3640

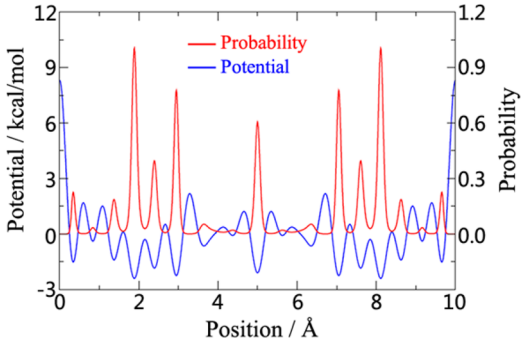

Figure 4. Rough potential energy surface (blue) from the sum of 10 Fourier cosine functions and the corresponding distribution probability (red) of the system positions under Boltzmann statistics at T = 300K.

is again compared between PICG-REMD and conventional REMD, which exchanges configurations between replicas at different temperatures. As noted earlier, the quantum effects can also be improved by using an artificial Planck constant of $\hbar' = \gamma\hbar$ ($\gamma > 1.0$) to further enhance the sampling in the PICG-REMD. To properly compare these two methods, both simulations used 16 replicas, and the parameters were optimized so that the exchange acceptances rates are at least 80% for every neighboring pairs of replicas. In REMD the highest temperature was chosen to be 800 K, while in PICG-REMD the values of P = 8 and γ = 2.5 were selected. The differences between the results from different sampling methods, with the analytical solution as the benchmark, are plotted in Figure 5. It is seen that both

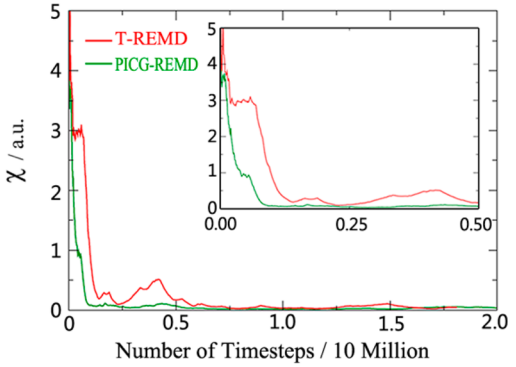

Figure 5. Convergence quantity χ for 20 million time steps of the simulations for the 1-D rough potential surface. The χ value from PICG-REMD (green) decays significantly faster than that from standard temperature REMD (red). (inset) A comparison of two χ quantities for the first five million time steps.

PICG-REMD and REMD can obtain comparable results with the Boltzmann distribution, but the PICG-REMD obtains the correct results in a more efficient way. It is again evident that the PICG-REMD result is smoother. The larger number of jumps found in the REMD trajectory (Figure 6) indicates that the REMD method is still affected by the trapping issue. However, PICG-REMD can reach the convergent results more smoothly in about one million time steps.

Additional insight can be gained by examining how these two methods work to overcome the free energy barriers. In general, the REMD method smoothes the free energy surface of the top, most-elevated temperature replica. Comparison between the modified free energy surfaces of the conventional REMD method

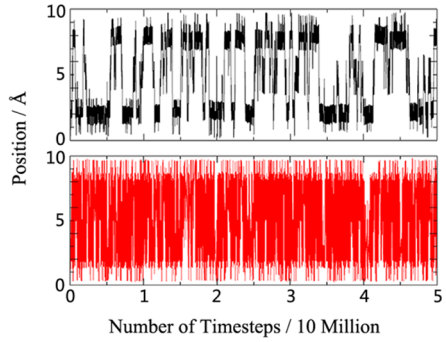

Figure 6. Position trajectories of the particle under the 1-D rough potential surface from 50 million time steps of standard temperature REMD (black) and PICG-REMD (red).

and the PICG-REMD provide more insights about the high sampling efficiency of the PICG-REMD method. These results are shown in Figure 7. For the conventional REMD, the free energy barriers can be reduced by gradually increasing the temperature, and the largest free energy barrier is reduced from ∼4.5 to ∼1.5 kcal mol^{-1}. However, the free energy surface is biased much more significantly by the quantum effects in PICG-REMD. Not only can the tunneling reduce the energy barriers on the free energy surface but also it can shift the positions of the minima. As the quantum effect becomes stronger, two neighboring minima may even collapse together and merge into a single minimum. The overall free energy surface is extensively smoothed out and becomes much flatter than the classical free energy surface. As a result of the quantum tunneling, some barriers present in the classical free energy surfaces are completely flattened in the quantum free energy surfaces.

3.2. Alanine Dipeptide. PICG-REMD simulations were also conducted for alanine dipeptide, which is a small biomolecular system and often used as a test case in sampling methods development. Two backbone dihedral torsions, φ and ϕ, of this dipeptide compose the elementary structure that is essential for the protein backbone conformations. The free energy surface along the two correlated dihedral torsions has attracted interest from experimental and theoretical researchers for many years.[33,34] For example, high-accuracy electronic structure calculations have been conducted to construct the potential energy surfaces and free energy surfaces for its conformational changes.[35,36] In molecular modeling, additional cross-term corrections are applied to the dipeptide backbone to better represent the accurate backbone structures or folding/unfolding processes for proteins by empirical force fields.[37] However, an accurate calculation of the two-dimensional (2-D) free energy surface in the (ϕ, φ) plane is still challenging, because this free energy surface is very rough, and the dihedral torsion is a relatively slow motion compared with other degrees of freedom in the system (i.e., bond stretching). Several important free energy minima cannot be found from the conventional MD simulations, and the corresponding free energy barriers are also hard to estimate.

The goal here is to illustrate that PICG-REMD can explore much larger conformational spaces for biomolecules than can conventional MD simulations, and that the PICG-REMD method is able to capture the important structures and corresponding free energies. We are aiming here neither to compare the accuracy of the free energy surface with quantum mechanical calculations nor to compare with the methods using biased potentials such as umbrella-sampling technique, which will be

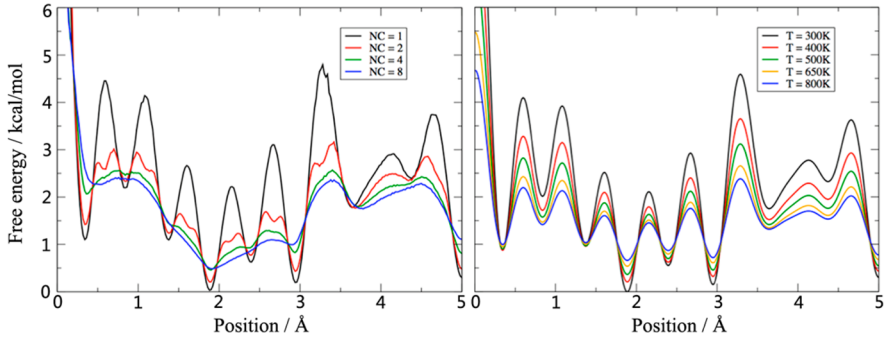

Figure 7. Free energy surfaces calculated from different simulation replicas of PICG-REMD (left) and standard temperature REMD (right). The PICG-REMD replicas can significantly smooth the free energy surface by quantum tunneling and delocalization effects.

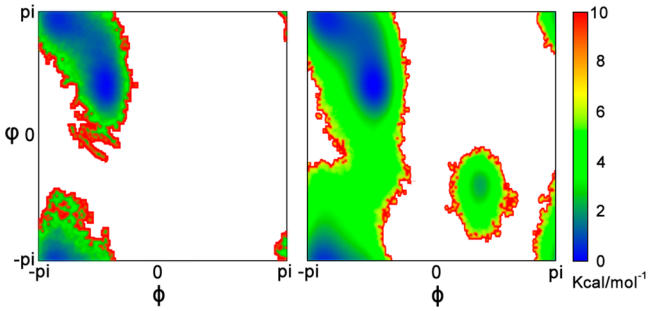

Figure 8. 2-D free energy surface for the $\varphi-\phi$ backbone torsions in alanine dipeptide. Compared to the conventional MD (left), PICG-REMD (right) is able to obtain all important configurations of this peptide.

presented elsewhere later as another study. The result is shown in Figure 8, with a comparison to the free energy surface from conventional MD simulations. Although in the conventional MD simulation the two important minima are well-sampled in the (ϕ, φ) plane for negative values of ϕ and values of φ around $-\pi$ or π, the barrier linking the two minima through the region of φ near $-\pi/2$ to 0 was not captured on the free energy surface. On the other hand, in the PICG-REMD calculation, not only is the wide energy barrier fully sampled but also a third minimum, located near $(\pi/2, -\pi/2)$, is clearly observed. It is therefore shown from this benchmark test that the smoothed free energy surfaces generated from a contraction (coarse-graining) of quantum path integrals enhances the sampling of the classical configuration distribution, for a complex all-atom system.

4. CONCLUDING REMARKS

In this study, we have presented and applied the PICG-REMD methodology, which couples NMPIMD quantum simulations at various levels of quasi-particle bead coarse-graining (contractions) in the potential evaluation through HREMD. In turn, this approach improves the sampling efficiency of the classical (centroid) replica via an effective incorporation of quantum effects such as tunneling and delocalization. Using the contracted variables, the various replicas can possess different degrees of quantization. The exchange of configurations between different replicas is made periodically and then accepted according to the Metropolis criteria. Because of the quantum tunneling and delocalization effects, the free energy surface in the top replica is greatly smoothed, and the system is constantly switched between the classical (centroid) replica and quantum replicas of the particles. PICG-REMD was shown to enhance the sampling of a classical free energy surface without alteration, and by properly choosing parameters to control the degree of fictitious quantum effects and the exchange rates, the PICG-REMD approach can achieve a higher sampling efficiency compared to the conventional REMD method.

The PICG-REMD method has been validated in three different benchmark systems in the present paper, namely, (1) a 1-D oscillator in an asymmetric double-well potential, (2) a 1-D oscillator in a random potential from the sum of a series of cosine functions, and (3) an all-atom model of alanine dipeptide. The results from all of these three benchmarks show that PICG-REMD can be a useful new approach for efficiently sampling the free energy landscape of complex systems. Moreover, this approach should not be viewed as being in competition with standard temperature REMD or other forms of HREMD. Indeed, PICG-REMD can also be combined with other REMD methods to create highly scalable and powerful multidimensional replica-exchange algorithms.[38]

AUTHOR INFORMATION

Corresponding Author

*E-mail: gavoth@uchicago.edu.

Notes

The authors declare no competing financial interest.

ACKNOWLEDGMENTS

This research was supported by the National Science Foundation (NSF Grant No. CHE-1214087). We thank S.-g. Kang from Computational Biology Center, IBM Thomas J. Watson Research Center, NY for useful discussions for this research. Y.P. was supported by IBM through the Summer Intern Program. R.Z. acknowledges the support from IBM Blue Gene Science Program.

REFERENCES

(1) Dror, R. O.; Dirks, R. M.; Grossman, J. P.; Xu, H.; Shaw, D. E. Biomolecular Simulation: A Computational Microscope for Molecular Biology. *Annu. Rev. Biophys.* **2012**, *41*, 429−452.

(2) Zuckerman, D. M. Equilibrium Sampling in Biomolecular Simulations. *Annu. Rev. Biophys.* **2011**, *40*, 41−62.

(3) Adcock, S. A.; McCammon, J. A. Molecular Dynamics: Survey of Methods for Simulating the Activity of Proteins. *Chem. Rev.* **2006**, *106*, 1589−1615.

(4) Scheraga, H. A.; Khalili, M.; Liwo, A. Protein-Folding Dynamics: Overview of Molecular Simulation Techniques. *Annu. Rev. Phys. Chem.* **2007**, *58*, 57−83.

(5) Patey, G. N.; Valleau, J. P. A Monte Carlo Method for Obtaining the Interionic Potential of Mean Force in Ionic Solution. *J. Chem. Phys.* **1975**, *63*, 2334−2339.

(6) Valleau, J. P.; Card, D. N. Monte Carlo Estimation of the Free Energy by Multistage Sampling. *J. Chem. Phys.* **1972**, *57*, 5457−5462.
(7) Laio, A.; Parrinello, M. Escaping Free-Energy Minima. *Proc. Natl. Acad. Sci. U.S.A.* **2002**, *99*, 12562−12566.
(8) Kumar, S.; Bouzida, D.; Swendsen, R. H.; Kollman, P. A.; Rosenberg, J. M. The Weighted Histogram Analysis Method for Free-Energy Calculations on Biomolecules. I. The Method. *J. Comput. Chem.* **1992**, *13*, 1011−1021.
(9) Kumar, S.; Rosenberg, J. M.; Bouzida, D.; Swendsen, R. H.; Kollman, P. A. Multidimensional Free-Energy Calculations Using the Weighted Histogram Analysis Method. *J. Comput. Chem.* **1995**, *16*, 1339−1350.
(10) Park, S.; Schulten, K. Calculating Potentials of Mean Force from Steered Molecular Dynamics Simulations. *J. Chem. Phys.* **2004**, *120*, 5946−5961.
(11) Kirkpatrick, S.; Gelatt, C. D.; Vecchi, M. P. Optimization by Simulated Annealing. *Science* **1983**, *220*, 671−680.
(12) Maragliano, L.; Vanden-Eijnden, E. A Temperature Accelerated Method for Sampling Free Energy and Determining Reaction Pathways in Rare Events Simulations. *Chem. Phys. Lett.* **2006**, *426*, 168−175.
(13) Maragliano, L.; Vanden-Eijnden, E. Single-Sweep Methods for Free Energy Calculations. *J. Chem. Phys.* **2008**, *128*, 184110.
(14) Abrams, C. F.; Vanden-Eijnden, E. Large-Scale Conformational Sampling of Proteins Using Temperature-Accelerated Molecular Dynamics. *Proc. Natl. Acad. Sci. U.S.A.* **2010**, *107*, 4961−4966.
(15) Sugita, Y.; Okamoto, Y. Replica-Exchange Molecular Dynamics Method for Protein Folding. *Chem. Phys. Lett.* **1999**, *314*, 141−151.
(16) Zhou, R.; Berne, B. J.; Germain, R. The Free Energy Landscape for Beta Hairpin Folding in Explicit Water. *Proc. Natl. Acad. Sci. U.S.A.* **2001**, *98*, 14931−14936.
(17) Paschek, D.; García, A. E. Reversible Temperature and Pressure Denaturation of a Protein Fragment: A Replica Exchange Molecular Dynamics Simulation Study. *Phys. Rev. Lett.* **2004**, *93*, 238105.
(18) Fukunishi, H.; Watanabe, O.; Takada, S. On the Hamiltonian Replica Exchange Method for Efficient Sampling of Biomolecular Systems: Application to Protein Structure Prediction. *J. Chem. Phys.* **2002**, *116*, 9058−9067.
(19) Liu, P.; Kim, B.; Friesner, R. A.; Berne, B. J. Replica Exchange with Solute Tempering: A Method for Sampling Biological Systems in Explicit Water. *Proc. Natl. Acad. Sci. U.S.A.* **2005**, *102*, 13749−13754.
(20) Lyman, E.; Ytreberg, F. M.; Zuckerman, D. M. Resolution Exchange Simulation. *Phys. Rev. Lett.* **2006**, *96*, 028105.
(21) Li, H.; Yang, W. Sampling Enhancement for the Quantum Mechanical Potential Based Molecular Dynamics Simulations: A General Algorithm and Its Extension for Free Energy Calculation on Rugged Energy Surface. *J. Chem. Phys.* **2007**, *126*, 114104.
(22) Okur, A.; Roe, D. R.; Cui, G.; Hornak, V.; Simmerling, C. Improving Convergence of Replica-Exchange Simulations through Coupling to a High-Temperature Structure Reservoir. *J. Chem. Theory Comput.* **2007**, *3*, 557−568.
(23) Lyman, E.; Zuckerman, D. M. Ensemble-Based Convergence Analysis of Biomolecular Trajectories. *Biophys. J.* **2006**, *91*, 164−172.
(24) Li, H.; Li, G.; Berg, B. A.; Yang, W. Finite Reservoir Replica Exchange to Enhance Canonical Sampling in Rugged Energy Surfaces. *J. Chem. Phys.* **2006**, *125*, 144902.
(25) Liu, P.; Berne, B. J. Quantum Path Minimization: An Efficient Method for Global Optimization. *J. Chem. Phys.* **2003**, *118*, 2999−3005.
(26) Lee, Y.-H.; Berne, B. J. Quantum Thermal Annealing with Renormalization: Application to a Frustrated Model Protein. *J. Phys. Chem. A* **2001**, *105*, 459−464.
(27) Santoro, G. E.; Martoňák, R.; Tosatti, E.; Car, R. Theory of Quantum Annealing of an Ising Spin Glass. *Science* **2002**, *295*, 2427−2430.
(28) Feynman, R. P.; Hibbs, A. R. *Quantum Mechanics and Path Integrals;* McGraw-Hill: New York, 1965.
(29) Cao, J.; Berne, B. J. A Born-Oppenheimer Approximation for Path Integrals with an Application to Electron Solvation in Polarizable Fluids. *J. Chem. Phys.* **1993**, *99*, 2902−2916.
(30) Cao, J.; Martyna, G. J. Adiabatic Path Integral Molecular Dynamics Methods. II. Algorithms. *J. Chem. Phys.* **1995**, *104*, 2028−2035.
(31) Cao, J.; Berne, B. J. Monte Carlo Methods for Accelerating Barrier Crossing: Anti-Force-Bias and Variable Step Algorithms. *J. Chem. Phys.* **1990**, *92*, 1980−1985.
(32) Zhou, R.; Berne, B. J. Smart Walking: A New Method for Boltzmann Sampling of Protein Conformations. *J. Chem. Phys.* **1997**, *107*, 9185−9196.
(33) Hermans, J. The Amino Acid Dipeptide: Small but Still Influential after 50 Years. *Proc. Natl. Acad. Sci. U.S.A.* **2011**, *108*, 3095−3096.
(34) Parchaňský, V.; Kapitán, J.; Kaminský, J.; Šebestík, J.; Bouř, P. Ramachandran Plot for Alanine Dipeptide as Determined from Raman Optical Activity. *J. Phys. Chem. Lett.* **2013**, *4*, 2763−2768.
(35) Smith, P. E. The Alanine Dipeptide Free Energy Surface in Solution. *J. Chem. Phys.* **1999**, *111*, 5568−5579.
(36) Tobiast, D. J.; Brooks, C. L., III Conformational Equilibrium in the Alanine Dipeptide in the Gas Phase and Aqueous Solution: A Comparison of Theoretical Results. *J. Phys. Chem.* **1992**, *96*, 3864−3870.
(37) Mackerell, A. D., Jr.; Feig, M.; Brooks, C. L., III Extending the Treatment of Backbone Energetics in Protein Force Fields: Limitations of Gas-Phase Quantum Mechanics in Reproducing Protein Conformational Distributions in Molecular Dynamics Simulations. *J. Comput. Chem.* **2004**, *25*, 1400−1415.
(38) Jiang, W.; Luo, Y.; Maragliano, L.; Roux, B. Calculation of Free Energy Landscape in Multi-Dimensions with Hamiltonian-Exchange Umbrella Sampling on Petascale Supercomputer. *J. Chem. Theory Comput.* **2012**, *8*, 4672−4680.